IEEE Access
Multidisciplinary | Rapid Review | Open Access Journal

Received October 4, 2020, accepted October 18, 2020, date of publication October 28, 2020, date of current version January 22, 2021.

Digital Object Identifier 10.1109/ACCESS.2020.3034361

Multi-Objective Design of Output LC Filter for Buck Converter via the Coevolving-AMOSA Algorithm

XINZE LI[1], (Student Member, IEEE), XIN ZHANG[2,3], (Senior Member, IEEE), AND FANFAN LIN[4], (Student Member, IEEE)

[1]School of Electrical and Electronic Engineering, Nanyang Technological University, Singapore 639798
[2]College of Electrical Engineering, Zhejiang University, Hangzhou 310027, China
[3]Hangzhou Global Scientific and Technological Innovation Center, Zhejiang University, Hangzhou 310058, China
[4]ERI@N, Interdisciplinary Graduate Programme, Nanyang Technological University, Singapore 639798

Corresponding author: Xin Zhang (zhangxin_ieee@163.com)

This work was supported by the Start-up Fund of Zhejiang University.

ABSTRACT Output *LC* filter is one of the most important parts for Buck converters. The existing optimization methods for *LC* filter fail to provide a fully optimized design. The difficulty in a holistic design approach lies in the trade-off relationships among different design targets. For example, smaller volume results in worse filtering capability and lower efficiency. To improve the overall performance of the output *LC* filter in Buck converter, a multi-objective design is proposed, taking the power loss, cut-off frequency and volume as design targets. This proposed holistic design approach utilizes Pareto-Frontier to achieve a compact *LC* filter with optimized efficiency and filtering capability. However, Pareto-Frontier generated by the previous multi-objective algorithms suffers from nonuniform or incomplete coverage, which seriously undermines design accuracy. Thus, the coevolving-AMOSA algorithm is proposed to provide a Pareto-Frontier with uniform and complete coverage. Via this proposed multi-objective design for the output *LC* filter in Buck converter with the coevolving-AMOSA algorithm, output *LC* filter can be flexibly designed to meet requirements in various applications while maintaining outstanding comprehensive performance. Optimal design cases for three specific application scenarios are presented as examples. Finally, the experimental results validate the effectiveness of the proposed multi-objective approach.

INDEX TERMS Output *LC* filter, multi-objective design, Pareto-Frontier, coevolving-AMOSA.

I. INTRODUCTION

Buck converters are playing important roles in both industries and our daily life. In industry, Buck converters are applied in electric vehicles [1], renewable energy systems [2], and others [3] for power regulation and voltage conversion [4]. In our daily life, the applications of Buck converters are everywhere, such as portable electronic devices [5], power audio systems [6], photovoltaic systems [7], etc.

To reduce the ripples of Buck converters, passive output *LC* filter is commonly accepted, due to its low cost and easy implementation. Traditional design [8] of output *LC* filter mainly relies on the output voltage and current ripple requirements. However, output *LC* filter not only has influence on the ripples of output voltage and current, but also affects other performance [9] of Buck converters. For example, the parameter selection of *LC* filter will directly affect the power loss of Buck converter which is expected to be as small as possible to maintain high power efficiency. Moreover, the values of inductance and capacitance will influence the volume of *LC* filter. Additionally, to ensure better filtering capability, the cut-off frequency is required to be small, which is also determined by the parameters of output *LC* filter.

Apparently, some specific applications have strict requirements on certain design objectives. As described in Fig. 1, airplanes, satellites and electric vehicles demand high-efficiency products [10]. Battery adapter, rooftop PV, digital camera and LED, which have limited space, prefer more compact electronic devices [11]. And the *LC* filter with smaller cut-off frequency in Buck converter displays better filtering capability, which is suitable for audio amplifier or MP3 player with strict requirements on the ripple reduction [6]. Even though some specific applications have strict requirements on certain performance indicators, the overall performance of Buck converter is still expected to be optimal, which means other design objectives should also be taken into considerations.

The associate editor coordinating the review of this manuscript and approving it for publication was Ahmad Elkhateb.

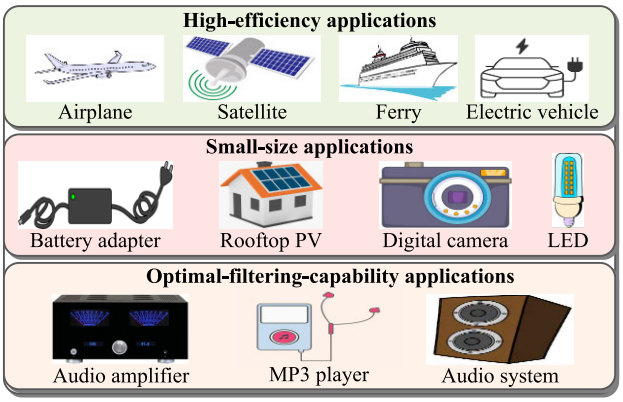

FIGURE 1. Descriptions of requirements of different applications on Buck converters.

However, the literature survey reveals numerous research publications on the design of *LC* filter which only deals with one design objective, such as cost [12], volume [13], voltage quality [14] and reliability [15]. For instance, the volume of the capacitor is set as the design objective in [13]. To improve power efficiency, power loss is optimized in [16]. For optimal filtering performance, cut-off frequency is considered in [17].

The difficulty in conducting the multi-objective design for the *LC* filter in Buck converter lies in the trade-off relationships among different design objectives. For example, smaller volume requires smaller values of inductance and capacitance, resulting in larger power loss and worse filtering capability [16]. It is admitted that there are some researchers working on the multi-objective optimization for the *LC* filter in Buck converter such as [9], [14] and [18]. Whereas power efficiency is neglected in these research works which is of great significance for energy saving and environmental friendliness. **Therefore, to conduct the multi-objective design considering the power efficiency, filtering capability and volume for the*LC*filter in Buck converter is the first challenge of this article.**

Additionally, to solve the multi-objective design problems, usually multi-objective optimization algorithms are adopted to locate Pareto-Frontier which is composed of all optimal solutions. Multi-objective algorithms incorporate three main types: indicator-based algorithms, decomposition-based algorithms, and population-based algorithms. Indicator-based algorithms adopt indicator functions to obtain Pareto-Frontier. Decomposition-based algorithms decompose the original multi-objective problem into several single objective problems and solve them to obtain Pareto-Frontier. Population-based multi-objective algorithms evaluate multiple solutions (which form the population) at one time, and thus can quickly obtain Pareto-Frontier. The commonly used multi-objective algorithms include NSGA-II [19], MOPSO [20], AMOSA [21], MOEA/D [22], and IBEA [22]. However, the existing multi-objective algorithms suffer from the nonuniform or incomplete coverage of Pareto-Frontier, seriously undermining the design accuracy [23]. **Thus, the second challenge of this article to conduct the multi-objective design for the*LC*filter in Buck converter is to improve the uniformity and completeness of Pareto-Frontier for more accurate and fully-optimized designs.**

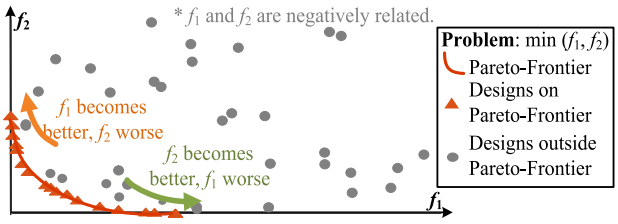

FIGURE 2. Example of Pareto-Frontier for the minimization of f_1 and f_2.

Therefore, in this article, a multi-objective design approach for the output *LC* filter in Buck converter with coevolving-AMOSA algorithm is proposed to achieve a fully-optimized *LC* filter. In Stage 1, power efficiency, cut-off frequency and volume as three design objectives are analyzed. And in Stage 2, the specially proposed coevolving-AMOSA algorithm is adopted for this multi-objective design approach to locate Pareto-Frontier accurately. Then in Stage 3, the final design solutions can be selected along the obtained Pareto-Frontier according to the application requirements. In this article, three design cases which fit three specific application scenarios will be provided as design examples.

The rest of the paper is organized as follows. In Section II, problem descriptions will be provided, regarding the trade-off relationships among the three design objectives and the nonuniform and incomplete Pareto-Frontier obtained by common multi-objective algorithms. Detailed analysis of the three design objectives, power efficiency, cut-off frequency and volume will be offered in Section III. The proposed multi-objective design approach for the *LC* filter in Buck converter with the coevolving-AMOSA algorithm is detailly introduced in Section IV. Three design examples are listed in Section V, and the corresponding experimental verification are given in Section VI. Finally, conclusion is summarized.

II. PROBLEM DESCRIPTIONS FOR THE MULTI-OBJECTIVE DESIGN OF THE OUTPUT LC FILTER IN BUCK CONVERTER

A. PRELIMINARIES: INTRODUCTION TO PARETO-FRONTIER

When several conflicting objectives are considered, it is impossible to reach one global optimal design with the optimization of all the objectives, since the optimization of some objectives will sacrifice others. Thus, Pareto optimum is defined for a solution if there is no change that could lead to improvements of all objectives [24]. And Pareto-Frontier is composed of all Pareto optima for this multi-objective optimization problem. There exists no design that can be better than the designs on the Pareto-Frontier in all objectives. An example of Pareto-Frontier for the minimization of f_1 and f_2 is given in Fig. 2 where f_1 and f_2 are negatively related.

In a word, when objectives are in trade-off relationships, Pareto-Frontier provides optimal designs, based on which the optimal multi-objective designs for *LC* filter can be obtained. With considerations of various application requirements, one final design solution along Pareto-Frontier can be picked out.

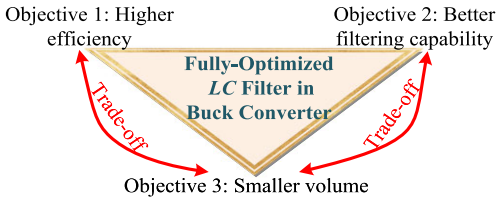

FIGURE 3. Descriptions of the multi-objective design for the *LC* filter in Buck converter in this article.

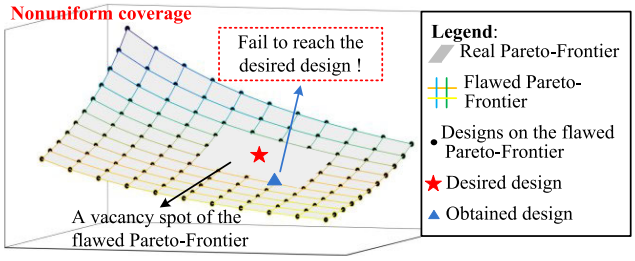

FIGURE 4. Problem description: nonuniform coverage of Pareto-Frontier.

B. PROBLEM I: TRADE-OFF RELATIONSHIPS AMONG THE THREE DESIGN OBJECTIVES FOR THE OUTPUT LC FILTER IN BUCK CONVERTER

To guarantee a holistic performance, more comprehensive design objectives should be considered for the optimization of the output *LC* filter in Buck converter. Power efficiency, cut-off frequency and volume are taken into account in this article to realize a compact *LC* filter with optimized efficiency and filtering capability for Buck converter.

However, as described in Fig. 3, there are trade-off relationships between these three objectives. The minimization of power loss is contradicting with smaller volume, and the minimization of volume contradicts with smaller cut-off frequency, which means smaller volume will lead to worse efficiency and filtering capability.

Targeted at this problem, the first challenge of this article is to deal with the conflicting relationships among the three design objectives (power loss, cut-off frequency and volume) to realize a fully optimized output *LC* filter for Buck converter.

C. PROBLEM II: THE NONUNIFORM AND INCOMPLETE COVERAGE OF PARETO-FRONTIER

As introduced in Section II-A, Pareto-Frontier is usually utilized to realize the optimization of multiple conflicting design objectives. And the multi-objective optimization algorithms can be adopted to obtain Pareto-Frontier. However, the Pareto-Frontier obtained by the commonly-used multi-objective optimization algorithms suffers from the following two drawbacks.

The first drawback is the nonuniform coverage of the Pareto-Frontier, as displayed in Fig. 4. The obtained Pareto-Frontier fails to cover the area uniformly, resulting in one or more vacant areas. If desired *LC* filter design is in the vacant position, the final obtained design solution will differ from the desired design solution, deteriorating the design accuracy.

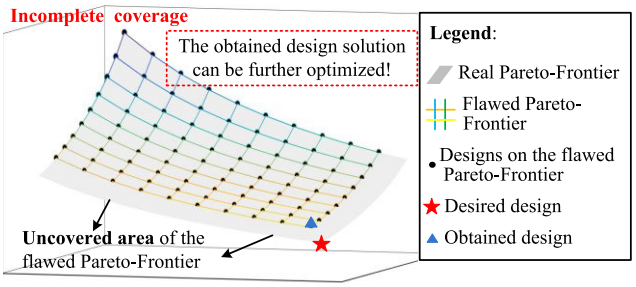

FIGURE 5. Problem description: incomplete coverage of Pareto-Frontier.

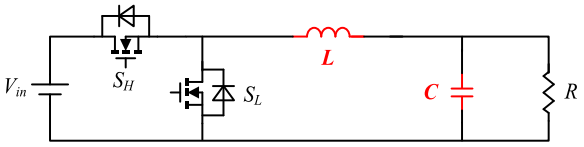

FIGURE 6. Circuit diagram of the synchronous Buck converter.

The second drawback is the incomplete coverage of the Pareto-Frontier, as displayed in Fig. 5. Under this case, the Pareto-Frontier obtained by the existing multi-objective optimization algorithms has too small and incomplete coverage. Thus, the obtained design solution is probably not a fully optimized one, negatively affecting the performance of the designed *LC* filter.

Both drawbacks of the Pareto-Frontier discussed above, the nonuniform and incomplete coverage, are expected to be avoided to ensure an accurate and fully optimized design for the output *LC* filter in Buck converter. Thus, the second challenge of this article is to improve the uniformity and completeness of Pareto-Frontier.

III. ANALYSIS OF THE THREE DESIGN OBJECTIVES FOR LC FILTER: POWER EFFICIENCY, CUT-OFF FREQUENCY AND VOLUME

A. ANALYSIS OF DESIGN OBJECTIVE 1: OPTIMIZED TOTAL POWER LOSS FOR THE BUCK CONVERTER OF OPTIMAL POWER EFFICIENCY

Since the designed output *LC* filter will affect the total power loss of the whole Buck converter, the total power loss of Buck converter is set as the first design objective.

The circuit diagram of synchronous Buck converter is shown in Fig. 6. According to [25]–[27], total power loss includes the power losses of switches S_L and S_H (S_L and S_H are defined in Fig. 6) and the power losses of *LC* filters. In this article, the designable parameters are the values of inductance L and capacitance C, and so the power losses are expressed in terms of whether they are related to L and C, as the following.

1) DRIVING LOSS OF SWITCHES S_L AND S_H (P_{L_DR})

Driving loss P_{l_dr} [27] is defined in (1):

$$P_{l\_dr} = 2Q_G V_{gs} f \tag{1}$$

where Q_G is the total gate charge of main switches, V_{gs} is the gate-to-source voltage and f is the switching frequency. P_{l_dr} is constant, since Q_G, V_{gs} and f are fixed design specifications.

2) CONDUCTION LOSS OF SWITCHES S_L AND S_H (P_{L_ON}(L))

With [27], the conduction loss of S_L and S_H, is expressed as:

$$P_{l\_on}(L) = DR_{on}(\frac{1}{12}(\frac{V_{in}-V_o}{Lf}D)^2 + I_o^2) \tag{2}$$

where V_{in}, V_o are the input and output voltages. I_o is the output current. D is the duty cycle of high-side switch S_H. R_{on} is the equivalent drain-source on resistance of switches. P_{l_on} relates to L, according to (2), in which V_o, I_o, D, R_{on} are constant design specifications.

3) SWITCHING LOSS OF SWITCHES S_L AND S_H (P_{L_S})

The switching loss P_{l_s} of switches S_H and S_L is in (3) [27]:

$$P_{l\_s} = 0.5V_{in}I_L\left(t_{r\_H}+t_{f\_H}\right)f + 0.5V_{SD}I_L\left(t_{r\_L}+t_{f\_L}\right)f \tag{3}$$

where t_{r_H} and t_{f_H} are the rising and falling time of the high side switch S_H. t_{r_L} and t_{f_L} are the rising and falling time of the low side switch S_L. V_{SD} is the conduction voltage across the diode of S_L. As can be seen from (3), P_{l_s} is constant.

4) CORE LOSS OF INDUCTOR (P_{L_FE}(L))

According to [26], the core loss of inductor in Buck converter is computed by the Steinmetz equation:

$$P_{l\_Fe}(L) = k\Delta B^{\beta}f^{\alpha}\left[(D)^{1-\alpha} + (1-D)^{1-\alpha}\right]Vol_L(L) \tag{4}$$

where k, α, β are the parameters in the Steinmetz equation and are constants when the inductor core material is selected. ΔB is the magnetic fluctuation, calculated by [26] and datasheets of inductor cores. From (4), P_{l_Fe} only relates to inductance L.

5) COPPER LOSS OF INDUCTOR (P_{L_CU}(L))

The calculation of copper loss of inductor [25] is in (5):

$$P_{l\_Cu}(L) = (R_{dc}+R_{ac})(\frac{1}{12}(\frac{V_{in}-V_o}{Lf}D)^2 + I_o^2) \tag{5}$$

where R_{dc} is the dc winding resistance of inductor and is obtained from inductor datasheets, and R_{ac} is the ac winding resistance considering skin and proximity effects and is computed with [25]. From (5), P_{l_Cu} is related to L only.

6) POWER LOSS OF CAPACITOR (P_{L_C}(L, C))

The loss of capacitor is computed by (6), where I_{Ck} is the root mean square of the k^{th} harmonic current on the capacitor, and is related to both L and C [18]. tanδ is constant and can be found from the datasheets of capacitors. According to (6), with the increasing values of L and C, P_{l_C} decreases.

$$P_{l\_C}(L, C) = \sum_{k}^{\infty} I_{Ck}^2 \cdot \frac{\tan\delta}{2\pi kfC} \tag{6}$$

7) TOTAL POWER LOSS (P_{L_TOT}(L, C))

The total power loss sums (1) to (6) together, as shown in (7). According to (7) and Fig. 7, P_{l_tot} relates to both inductance L and capacitance C.

$$P_{l\_tot}(L, C) = P_{l\_dr} + P_{l\_s} + P_{l\_on}(L) + P_{l\_Cu}(L) + P_{l\_Fe}(L) + P_{l\_C}(L, C) \tag{7}$$

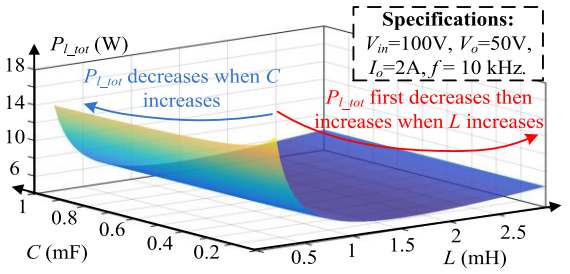

FIGURE 7. Effects of L and C on total power loss P_{l_tot}.

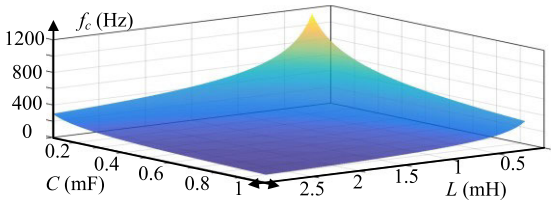

FIGURE 8. Effects of L and C on cut-off frequency f_c.

Since the minimization of total power loss is equivalent to the maximization of efficiency, the total power loss is required to be as small as possible. Thus, **the design objective 1 is to minimize total power loss for the design of the Buck converter with optimized power efficiency**.

B. ANALYSIS OF DESIGN OBJECTIVE 2: OPTIMIZED CUT-OFF FREQUENCY FOR THE BUCK CONVERTER WITH OPTIMAL FILTERING CAPABILITY

For the output LC filter in Buck converter, smaller cut-off frequency represents better filtering performance [18]. The relationships between f_c and L, C are shown in Fig. 8 and (8). **The design objective 2 is to minimize cut-off frequency for the Buck converter with optimized filtering capability**.

$$f_c(L, C) = \frac{1}{2\pi\sqrt{LC}} \tag{8}$$

C. ANALYSIS OF DESIGN OBJECTIVE 3: OPTIMAL VOLUME FOR A COMPACT BUCK CONVERTER

The size of Buck converter is an important factor to be considered in space-restricted applications [28]. In this article, since the design parameters are L and C, only the volume of inductor and capacitor is considered, and other volume such as the volume of cooling system is regarded as constant.

The relationship (9) between the inductor volume Vol_L and its inductance is deduced according to [18]:

$$Vol_L(L) = a_l \cdot L \tag{9}$$

where Vol_L is the inductor volume. a_l is computed by linear regression method. For instance, inductors of MCAP series of Multicomp with TAF-200 cores [30] are selected and shown in Fig. 9, in which statistical R^2 is close to 1, validating the linear relationship between Vol_L and L.

According to [18], the volume of capacitor Vol_C is linearly proportional to capacitance C, as (10) shows:

$$Vol_C(C) = a_c \cdot C \tag{10}$$

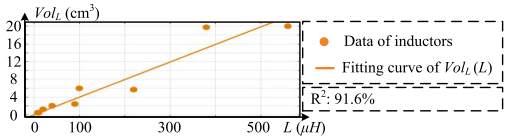

FIGURE 9. Effects of L on volumes of inductors Vol_L.

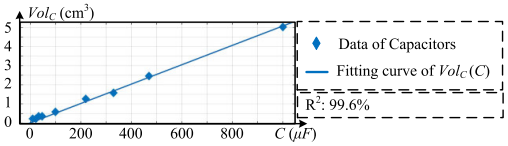

FIGURE 10. Effects of C on volumes of capacitors Vol_C.

where Vol_C is the capacitor volume. a_c can be computed by linear regression method. As an example, capacitors of ECA1JM series of Panasonic [31] are selected in Fig. 10, in which statistical R^2 is close to 1, validating the linear relationship between Vol_C and C.

With (9) and (10), the total volume V_{tot} to be minimized is shown in (11), and is linearly related to the inductance L and capacitance C. **The design objective 3 is to minimize the volume V_{tot} in (11) for a compact Buck converter**.

$$V_{tot}(L, C) = Vol_L(L) + Vol_C(C) = a_l \cdot L + a_c \cdot C \quad (11)$$

In summary, according to Fig. 7 to Fig. 10, as L and C increase, P_{l_tot} generally decreases, f_c decreases and V_{tot} increases. Thus, the minimization of volume V_{tot} is conflicting with the minimization of total power loss P_{l_tot} and cut-off frequency f_c.

IV. THE PROPOSED MULTI-OBJECTIVE DESIGN APPROACH FOR THE OUTPUT LC FILTER IN BUCK CONVERTER WITH COEVOLVING AMOSA ALGORITHM

In this article, aimed at solving problem I and problem II as discussed in Section II-B & C, a three-stage multi-objective design of output LC filter for Buck converter with the coevolving-AMOSA algorithm is proposed. The flowchart of the proposed design approach is described in Fig. 11.

A. STAGE 1: ANALYSIS OF THREE DESIGN OBJECTIVES

As described in the first part in Fig. 11, in Stage 1 of the proposed multi-objective design of output LC filter for Buck converter, three conflicting objectives (P_{l_tot}, f_c, V_{tot}) are detailly analyzed with respects to L and C.

Based on the design conditions, P_{l_tot} can be analyzed with (1) to (7) in Section III-A. f_c can obtained with (8) in Section III-B. And V_{tot} can be evaluated with (11) in Section III-C. At the end of Stage 1, three objective functions regarding P_{l_tot}, f_c and V_{tot} have been prepared for the multi-objective optimization in Stage 2.

B. STAGE 2: MULTI-OBJECTIVE OPTIMIZATION OF THE THREE DESIGN OBJECTIVES WITH COEVOLVING-AMOSA ALGORITHM

1) REALIZATION OF STAGE 2

With the three objective functions analyzed in Stage 1, the multi-objective optimization on these three design objectives will be conducted in Stage 2 with coevolving-AMOSA as

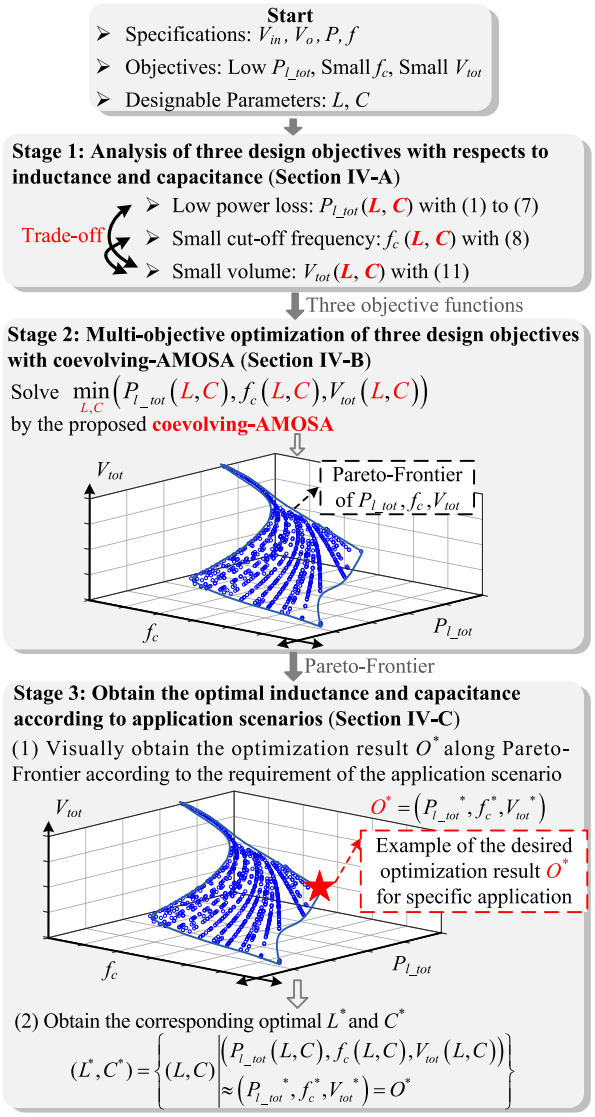

FIGURE 11. The proposed three-stage multi-objective design of output LC filter for Buck converter with the coevolving-AMOSA algorithm.

described in the second part of Fig. 11. The optimization function of this problem is given in (12) where $P_{l\_tot,\max}$, $f_{c,\max}$ and $V_{tot,\max}$ are defined as the limits of efficiency, cut-off frequency and size, respectively.

$$\begin{aligned} &\min_{L,C}(P_{l\_tot}(L, C), f_c(L, C), V_{tot}(L, C)) \\ &s.t.\ P_{l\_tot}(L, C) \le P_{l\_tot,\max} \\ &\quad f_c(L, C) \le f_{c,\max} \\ &\quad V_{tot}(L, C) \le V_{tot,\max} \end{aligned} \quad (12)$$

To solve (12), an improved AMOSA algorithm called the coevolving-AMOSA is utilized, which is introduced in Section IV-B-(b). The main reason why the AMOSA algorithm is adopted and modified is due to its faster computation speed compared with other multi-objective algorithms such as NSGA-II [19], MOPSO [20], IBEA [22], etc. With the proposed coevolving-AMOSA algorithm, a uniformly and completely covered Pareto-Frontier can be achieved. And then the obtained Pareto-Frontier will be delivered to Stage 3 for further selection of optimal design cases.

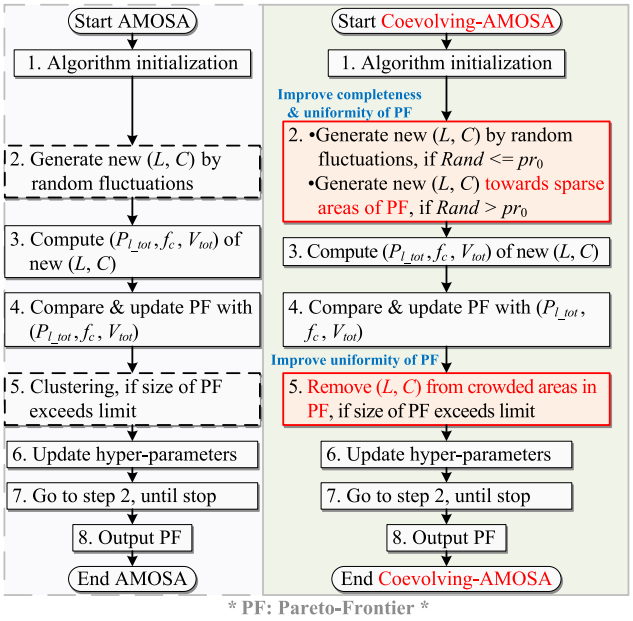

FIGURE 12. Flowcharts of the traditional AMOSA algorithm [21] and the proposed coevolving-AMOSA algorithm (in which PF represents Pareto-Frontier).

TABLE 1. Pseudo-Code of the Coevolving-AMOSA Algorithm.

Algorithm: the Coevolving-AMOSA
Initialize parameters of traditional AMOSA, coevolving probability pr_0, and PF to store optimal designs;
$Rand \leftarrow$ U(0, 1);
IF $pr_0 >= Rand$
Generate new (L,C) with random fluctuations;
ELSE
Generate new (L,C) towards sparse areas in PF;
Compute (P_{l_tot}, f_c, V_{tot}) with (1) - (11);
IF size of Pareto-Frontier exceeds limit
Randomly remove extra (L,C) from crowded areas in PF;
Update parameters of traditional AMOSA, decrease pr_0;
IF stop criterion is not met
Go to line 2
OUTPUT PF

2) THE PROPOSED COEVOLVING-AMOSA ALGORITHM

a: FLOWCHART OF THE PROPOSED COEVOLVING-AMOSA ALGORITHM

The flowchart of the proposed coevolving-AMOSA is compared with the traditional AMOSA [21] and shown in Fig. 12. The improvements of coevolving-AMOSA have been highlighted in red (step 2 and 5). The pseudo-code of the proposed coevolving-AMOSA is also given in Table 1, where U(0, 1) is the uniform distribution between [0, 1].

b: THE ADVANTAGES OF THE COEVOLVING-AMOSA: IMPROVE UNIFORMITY AND COMPLETENESS OF THE OBTAINED PARETO-FRONTIER

Compared with the traditional AMOSA, the coevolving-AMOSA algorithm can obtain the Pareto-Frontier which has better uniformity and completeness, so problems of Fig. 4 and 5 can be mitigated.

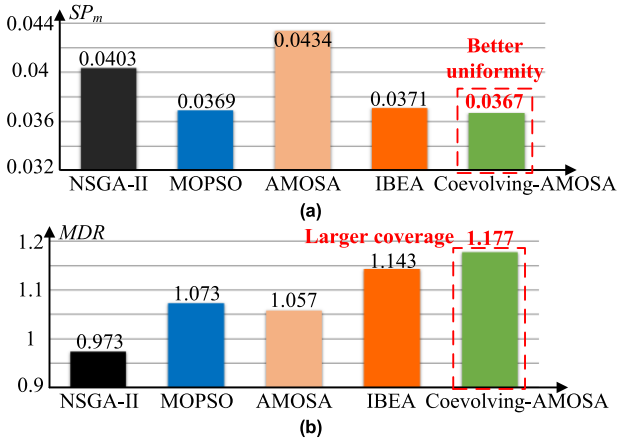

FIGURE 13. Expected performance of multi-objective algorithms: (a) SP_m; (b) *MDR*.

The first advantage, the better uniformity of the achieved Pareto-Frontier, benefits from both of the step 2 and step 5 in the proposed coevolving-AMOSA algorithm. In step 2, a coevolving probability pr_0 is introduced to control the process of new design (L, C) generation. During the iterations, pr_0 is decreasing from 1 to 0. If a random number is larger than pr_0, the generated new (L, C) will be led towards the sparse areas within Pareto-Frontier. And in step 5, extra designs (L, C) are randomly removed from crowded areas. With these two steps, uniformity of the obtained Pareto-Frontier can be greatly improved.

The second advantage, the better completeness of the achieved Pareto-Frontier, is attributable to step 2 in the coevolving-AMOSA algorithm. In step 2, if a random number is smaller than pr_0, the new (L, C) will be randomly generated, encouraging the algorithm to thoroughly search for the solution space to broaden the coverage, which benefits the completeness of the obtained Pareto-Frontier.

Therefore, with the uniform and complete Pareto-Frontier achieved by the coevolving-AMOSA algorithm, the multi-objective design for the output *LC* filter in Buck converter will be more accurate and fully optimized.

c: COMPARISONS BETWEEN THE PROPOSED COEVOLVING-AMOSA AND OTHER POPULAR MULTI-OBJECTIVE ALGORITHMS

In this part, several popular multi-objective evolutionary algorithms such as NSGA-II [19], MOPSO [20], traditional AMOSA [21] and some state-of-the-art algorithms such as IBEA [22] are given for comparison. Targeted at the multi-objective design in (12) for the output *LC* filter in Buck converter, these algorithms are repeated for 30 times. To indicate the uniformity and completeness of the Pareto-Frontier, two metrics are usually adopted: minimal spacing (SP_m), and maximum distribution range (*MDR*) [23]. Lower SP_m means better uniformity, and higher *MDR* means more complete coverage. Comparison results are listed in Fig. 13.

As shown in Fig. 13 (a), the traditional AMOSA is the worst in terms of uniformity due to its clustering step 5 in Fig. 12 [21]. With the proposed coevolving-AMOSA, SP_m becomes the smallest, indicating that it produces the most uniform Pareto-Frontier, even more uniform than the Pareto-Frontier generated with state-of-the-art IBEA.

As shown in Fig. 13 (b), *MDR* of NSGA-II is the lowest, meaning its coverage is far from satisfactory [29]. The coevolving-AMOSA displays its *MDR* at 1.177, so its Pareto-Frontier covers more complete area, providing fully-optimized design choices for engineers. From Fig. 13 (b), the coverage of the proposed coevolving-AMOSA is even wider and larger than the state-of-the-art algorithm IBEA.

To conclude, the proposed coevolving-AMOSA algorithm is able to generate a Pareto-Frontier with better uniformity and completeness, providing more accurate and fully optimized designs for the output *LC* filter in Buck converter.

C. STAGE 3: OBTAIN THE OPTIMAL DESIGN SOLUTION BASED ON APPLICATION REQUIREMENTS

With the Pareto-Frontier generated in Stage 2, Stage 3 of the proposed design approach is aimed to obtain the optimal L and C for specific application scenarios. As shown in Fig. 11, Stage 3 includes 2 steps, described as the followings.

In the beginning part of Stage 3, the optimization result $O^* = (P^*_{l\_tot}, f^*_c, V^*_{tot})$ is obtained visually along the Pareto-Frontier of three design objectives (power loss, cut-off frequency and volume) according to the requirement of application scenario.

After that, with the picked optimization result O^*, the corresponding optimal L^* and C^* are obtained by (13) to find the combination of L and C which can meet O^* best.

$$(L^*, C^*) = \left\{ (L, C) \left| \begin{array}{l} (P_{l\_tot}(L, C), f_c(L, C), V_{tot}(L, C)) \\ \approx \left(P^*_{l\_tot}, f^*_c, V^*_{tot}\right) = O^* \end{array} \right. \right\} \tag{13}$$

Overall, the final optimization solution of L^* and C^* can be achieved according to the specific requirement of application scenarios in Stage 3.

V. DESIGN EXAMPLES OF THE PROPOSED MULTI-OBJECTIVE DESIGN FOR THE OUTPUT LC FILTER IN BUCK CONVERTER WITH COEVOLVING-AMOSA ALGORITHM

A. DESIGN EXAMPLE WITH TRADITIONAL DESIGN METHOD [8]

$$L = \frac{(1 - D)V_o}{f \cdot I_o \cdot I_{ripple}} \tag{14}$$

$$C = \frac{(\pi + 4 \cdot \tan\delta) \cdot I_{ripple} \cdot I_o}{8\pi f \cdot V_o \cdot V_{ripple}} \tag{15}$$

For comparison with the proposed multi-objective design of the output *LC* filter for Buck converter, the traditional design is given here [8]. I_{ripple} and V_{ripple} are set as 40%, 10% respectively.

TABLE 2. Design Specifications of Design Examples.

Parameters of main circuit			
P_o	100 W	f	10 kHz
V_{in}	100 V	V_o	50 V
Main switches (C2M0080120D)			
Q_g	62 nC	V_{gs}	20 V
R_{on}	80 $m\Omega$	V_{SD}	4.3V
Output *LC* filter			
Inductor cores	TAF-200 series		
Capacitor	100V ECA1JM series of Panasonic		

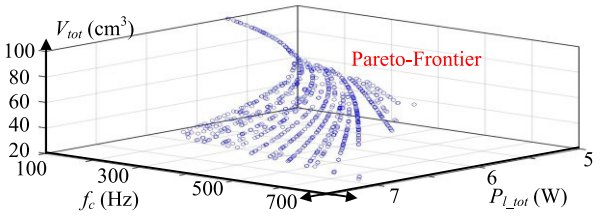

FIGURE 14. Visualized Pareto-Frontier of power loss, cut-off frequency and volume, where each blue dot represents an optimal design case.

With (14), the inductance is computed as 3.13mH [8]. According to (14), the capacitance of the traditional design is computed as 30μF [8]. P_{l_tot}, f_c and V_{tot} of the traditional design are evaluated as 6.5W, 495Hz and 122cm^3.

B. DESIGN EXAMPLES WITH THE PROPOSED MULTI-OBJECTIVE DESIGN OF OUTPUT LC FILTER FOR BUCK CONVERTER WITH COEVOLVING-AMOSA ALGORITHM

1) STAGE 1 OF THE DESIGN EXAMPLES

The design specifications are listed in Table 2. Three objectives with respects to L and C can be analyzed with (1) to (11), and are summarized as the following:

- *Objective*-1: minimize P_{l_tot} for the design of high-efficiency Buck converter based on (1) – (7);
- *Objective*-2: minimize f_c for the design of a Buck converter with optimal filtering capability based on (8);
- *Objective*-3: minimize V_{tot} for the design of a compact Buck converter based on (9) – (11).

C. (B) STAGE 2 OF THE DESIGN EXAMPLES

With the three design objective functions analyzed in Stage 1, the multi-objective design problem can be summarized in (12), in which the $P_{l\_tot,\max}$ is set as 10W, $f_{c,\max}$ is set as 700Hz, and $V_{tot,\max}$ is set as 100cm^3.

By following the pseudo-code of the proposed coevolving-AMOSA algorithm in Table 1, the Pareto-Frontier of power loss, cut-off frequency, and volume is generated, as shown in Fig. 14.

1) STAGE 3 OF THE DESIGN EXAMPLES

In Stage 3, based on the three specific application scenarios in Fig. 1, the following design cases are taken as examples.

Case 1: Minimize total power loss for the design of high-efficiency Buck converter. Case 1 is suitable for applications such as airplane, satellite, ferry, etc.

Case 2: Keep the same efficiency as the traditional design, while minimizing volume for the design of a compact

TABLE 3. Objective Values of the Three Required Optimal Designs.

	$P_{l\_tot}^*$ (W)	f_c^* (Hz)	V_{tot}^* (cm^3)
Optimal Case 1	5.18	146	63.4
Optimal Case 2	6.46	323	29.1
Optimal Case 3	5.7	103	100.0

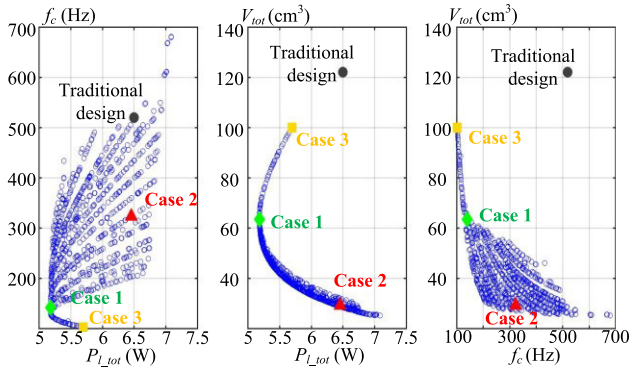

FIGURE 15. Projected Pareto-Frontier (blue points): (a) power loss vs. cut-off frequency; (b) power loss vs. volume; (c) cut-off frequency vs. volume.

TABLE 4. Inductance and Capacitance of Three Optimal Designs.

	Inductance L^* (mH)	Capacitance C^* (μF)
Optimal Design Case 1	1.49	800
Optimal Design Case 2	0.688	352
Optimal Design Case 3	2.41	1000

Buck converter. Case 2 is appropriate for space-constrained portable devices such as battery adapter, rooftop PV, digital camera, LED, etc.

Case 3: Minimize cut-off frequency for the design of the Buck converter with optimal filtering capability. Case 3 is applicable to areas like power audio amplifier, MP3 player, audio systems which have stricter requirements on the reduction of ripples.

Optimization results O^* of the three design cases, which consist of $P_{l\_tot}^*, f_c^*$ and V_{tot}^*, are visually obtained from the Pareto-Frontier in Fig. 14 and listed in Table 3.

For better visualization, the 3-D Pareto-Frontier in Fig. 14 is projected into three 2-D plots, as shown in Fig. 15, together with the traditional design and three optimal design cases. As shown in Fig. 15, compared to the traditional design, case 1 minimizes power loss by 1.32W, case 2 keeps the same efficiency as traditional design, while minimizing volume by 92.9cm^3, and case 3 minimizes the cut-off frequency by 392Hz.

After that, with (13) and the optimization results O^* of the three design cases in Table 3, the corresponding optimization solutions L^* and C^* are obtained and listed in Table 4.

VI. EXPERIMENTAL VERIFICATIONS

To validate the feasibility and effectiveness of the proposed multi-objective design approach for the output *LC* filter in Buck converter with coevolving-AMOSA algorithm, the design examples given in Table 4 in Section V are verified with hardware experiments in this section. The hardware main circuit is shown in Fig. 16. The detailed hardware

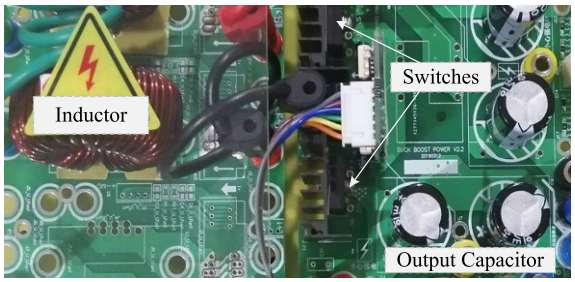

FIGURE 16. Main circuit of the designed synchronous Buck converter.

TABLE 5. Hardware Realization of the Three Required Optimal Designs.

Inductors of Optimal Design Cases				
Cases	L^*	**Core**	**Wire**	N
Case 1	1.49mH	T200B-75-200	UEFN/U 1mm	97
Case 2	688μH	T175-75-200	UEFN/U 1mm	81
Case 3	2.41mH	T250-75-200	UEFN/U 1mm	100
Capacitors of Optimal Design Cases				
Cases	C^*	**Realization**		
Case 1	800μF	Parallel: 330μF & 470μF, 100V ECA1JM		
Case 2	352μF	Parallel: 22μF & 330μF, 100V ECA1JM		
Case 3	1000μF	Single: 1000μF, 100V ECA1JM		

realization of Table 4 is shown in Table 5. The design specifications are the same as those in Table 2.

A. EXPERIMENTAL WAVEFORMS OF THE TRADITIONAL DESIGN CASE AND THREE OPTIMAL DESIGN CASES

The experimental waveforms of the traditional design case illustrated in Section V-A are given in Fig. 17 (a). And the three optimal design cases with the proposed multi-objective design approach of output *LC* filter in Buck Converter via coevolving-AMOSA algorithm illustrated in Section V-B are given in Fig. 17 (b) to (d) respectively.

B. EVALUATION OF THE EXPERIMENTAL RESULTS

The performance indicators of the traditional and three optimal design cases are evaluated in experiments and listed in Fig. 18 with respects to total power loss, cut-off frequency and volume. The detailed evaluations are stated as follows.

1) TRADITIONAL DESIGN CASE

With the traditional design approach introduced in Section V-A, the volume of the designed output *LC* filter in Buck converter is 123cm^3. The input power and output power are 97.9W and 91.1W respectively, and thus the total power loss is 6.8W and the efficiency is 93.05%. Its cut-off frequency is 490Hz.

2) OPTIMAL DESIGN CASE 1: MAXIMIZING EFFICIENCY

The optimal design case 1 as introduced in Section V-B-(c) is expected to have minimized power loss. The experimental results show that the optimal design case 1 has a volume at 59.6cm^3, 51.5% smaller than traditional design. Its input power and output power are 98.1W and 92.8W respectively, and thus the total power loss is 5.3W and the efficiency is 94.6%. This optimal design case 1 saves 1.6W loss compared with the traditional design case. Besides, its cut-off frequency

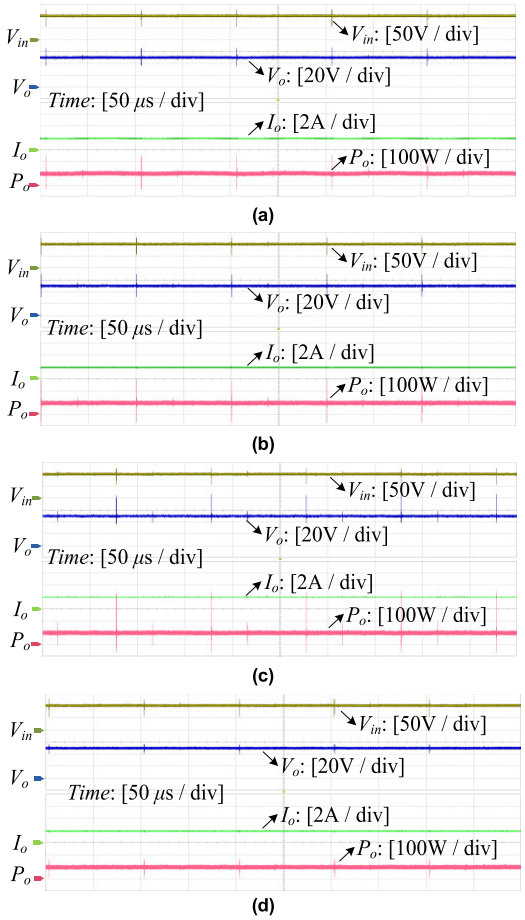

FIGURE 17. Waveforms of the design cases: (a) traditional design; (b) optimal design case 1; (c) optimal design case 2; (d) optimal design case 3.

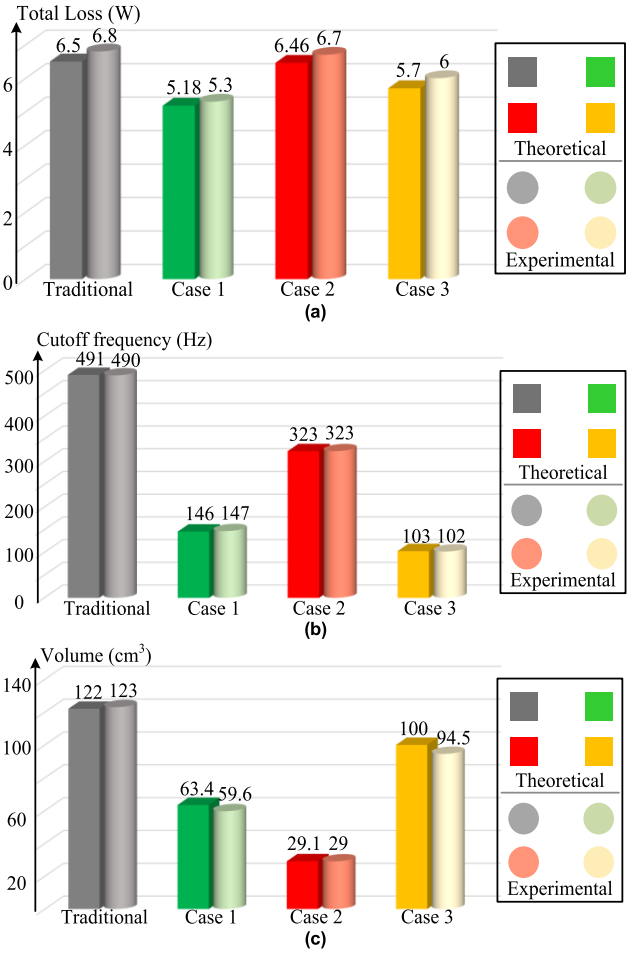

FIGURE 18. Experimental and theoretical results of the conventional and optimal design cases: (a) total power loss; (b) cut-off frequency; (c) volume.

is 147Hz. Therefore, the optimal design case 1 is suitable for high-efficiency applications in Fig. 1 like airplanes, electric vehicles, etc.

3) OPTIMAL DESIGN CASE 2: MINIMIZING VOLUME WHILE MAINTAINING SAME EFFICIENCY AS THE TRADITIONAL DESIGN

The optimal design case 2 as introduced in Section V-B-(c) is expected to have smaller volume while not sacrificing its power efficiency. The experimental results show that the optimal design case 2 has the input power and output power at 96.4W and 89.7W respectively, and thus the total power loss is 6.7W and the efficiency is 93.0%, almost the same as the traditional design case. Its volume is 29cm^3, 76.4% smaller than the traditional design. The cut-off frequency is 323Hz. Therefore, the optimal design case 2 is applicable to space-constrained portable devices such as battery adapters, rooftop PV, digital cameras, LED, etc.

4) OPTIMAL DESIGN CASE 3: MINIMIZING CUT-OFF FREQUENCY

The optimal design case 3 as introduced in Section V-B-(c) is expected to have minimized cut-off frequency for optimal filtering capability. The experimental results show that the optimal design case 3 has cut-off frequency at 102Hz, 79.2% lower than the traditional design. And its volume is 94.5cm^3, 23.2% smaller than traditional design. The input power and output power are 95.4W and 89.4W respectively, and thus the total loss is 6W and the efficiency is 93.7%, slightly better than traditional design. Therefore, the optimal design case 3 is suitable for audio systems in Fig. 1 such as power audio amplifiers and MP3 players which have stricter requirements on filtering capability.

Overall, the experimental results in Fig. 18 are in accordance with the theoretical analysis in Table 3, validating the feasibility and effectiveness of the proposed multi-objective design of output *LC* filter for Buck converter via the coevolving-AMOSA algorithm. The three optimal design cases perform better than the traditional design example in power efficiency, filtering capability and volume, validating the fully-optimized performance of the optimal designs with the proposed design method. And with the proposed multi-objective design approach, the output *LC* filters can be flexibly designed to meet different requirements in various application scenarios.

VII. CONCLUSION

In this article, a multi-objective design approach for the output *LC* filter in Buck converter via the coevolving-AMOSA

algorithm is proposed to deal with three conflicting design objectives, low power loss, better filtering capability, and small volume. This proposed design approach contains three stages. In the first stage, three design objectives with respects to inductance and capacitance (power loss, cut-off frequency and volume) will be analyzed detailly to generate three objective functions. And in Stage 2, the obtained three objective functions will be adopted for the multi-objective optimization by the coevolving-AMOSA algorithm to generate a Pareto-Frontier. Then in Stage 3, with the achieved Pareto-Frontier, the optimization result will be picked out along the Pareto-Frontier based on the concrete requirements of applications, and the final optimization solutions of optimal inductance and capacitance will be obtained. Specially, the coevolving-AMOSA algorithm is proposed for this multi-objective design approach and is utilized in Stage 2. The coevolving-AMOSA algorithm has been proved to have better uniformity and completeness of Pareto-Frontier than other algorithms, and thus the design solutions can be more accurate and fully optimized.

Three optimal design examples have been provided with the proposed multi-objective design approach for the output *LC* filter in Buck converter via the coevolving-AMOSA algorithm based on different requirements in three application scenarios. The optimized performance of these three optimal design examples has been verified through hardware experiments and compared with the design example by traditional design method. Thus, the feasibility and effectiveness of this proposed multi-objective design approach for the output *LC* filter in Buck converter with coevolving-AMOSA algorithm have been validated.

REFERENCES

[1] S.-K. Lim, H.-S. Lee, H.-R. Cha, and S.-J. Park, "Multi-level DC/DC converter for E-mobility charging stations," *IEEE Access*, vol. 8, pp. 48774–48783, 2020.

[2] H. U. R. Habib, S. Wang, M. R. Elkadeem, and M. F. Elmorshedy, "Design optimization and model predictive control of a standalone hybrid renewable energy system: A case study on a small residential load in Pakistan," *IEEE Access*, vol. 7, pp. 117369–117390, 2019.

[3] G. Zhang, N. Jin, L. Qu, and S. S. Yu, "Inherently non-pulsating input current DC-DC converter for battery storage systems," *IEEE Access*, vol. 8, pp. 140293–140302, 2020.

[4] H. You and X. Cai, "A three-level modular DC/DC converter applied in high voltage DC grid," *IEEE Access*, vol. 6, pp. 25448–25462, 2018.

[5] J. M. Martinez-Heredia, F. Colodro, J. L. Mora-Jimenez, A. Remujo, J. Soriano, and S. Esteban, "Development of GaN technology-based DC/DC converter for hybrid UAV," *IEEE Access*, vol. 8, pp. 88014–88025, 2020.

[6] M. Sobaszek, "Self-tuned Class-D audio amplifier with post-filter digital feedback implemented on digital signal controller," *IEEE Trans. Circuits Syst. I, Reg. Papers*, vol. 67, no. 3, pp. 797–805, Mar. 2020.

[7] B. Chandrasekar, C. Nallaperumal, S. Padmanaban, M. S. Bhaskar, J. B. Holm-Nielsen, Z. Leonowicz, and S. O. Masebinu, "Non-isolated high-gain triple port DC–DC buck-boost converter with positive output voltage for photovoltaic applications," *IEEE Access*, vol. 8, pp. 113649–113666, 2020.

[8] R. W. Erickson, *Fundamentals of Power Electronics*. New York, NY, USA: Chapman & Hall, 1997.

[9] A. De Nardo, N. Femia, G. Petrone, and G. Spagnuolo, "Optimal buck converter output filter design for point-of-load applications," *IEEE Trans. Ind. Electron.*, vol. 57, no. 4, pp. 1330–1341, Apr. 2010.

[10] J. Jiang, Z. Li, K. Song, B. Song, S. Dong, and C. Zhu, "A cascaded topology and control method for two-phase receivers of dynamic wireless power transfer systems," *IEEE Access*, vol. 8, pp. 47445–47455, 2020.

[11] L. Hu, X. Wei, Y. Luo, and J. Ma, "Synchronous high step-down ratio non-isolated LED constant current driver based on improved Watkins–Johnson topology," *IEEE Access*, vol. 7, pp. 18345–18353, 2019.

[12] R. Burkart and J. W. Kolar, "Component cost models for multi-objective optimizations of switched-mode power converters," in *Proc. IEEE Energy Convers. Congr. Expo.*, Denver, CO, USA, Sep. 2013, pp. 2139–2146.

[13] P. Pelletier, J.-M. Guichon, J.-L. Schanen, and D. Frey, "Optimization of a DC capacitor tank," *IEEE Trans. Ind. Appl.*, vol. 45, no. 2, pp. 880–886, Mar./Apr. 2009.

[14] D. O. Boillat, F. Krismer, and J. W. Kolar, "Design space analysis and ρ–η Pareto optimization of *LC* output filters for switch-mode AC power sources," *IEEE Trans. Power Electron.*, vol. 30, no. 12, pp. 6906–6923, Dec. 2015.

[15] H. Wang, M. Liserre, F. Blaabjerg, P. de Place Rimmen, J. B. Jacobsen, T. Kvisgaard, and J. Landkildehus, "Transitioning to physics-of-failure as a reliability driver in power electronics," *IEEE J. Emerg. Sel. Topics Power Electron.*, vol. 2, no. 1, pp. 97–114, Mar. 2014.

[16] X. Li, F. Lin, X. Zhang, M. Huang, and H. Wang, "Multi-objective design of LC filter for high-efficiency, High-power-density and high-performance buck converter," in *Proc. IEEE Energy Convers. Congr. Exposit. (ECCE)*, Baltimore, MD, USA, Sep. 2019, pp. 5132–5136.

[17] H. Kim and S.-K. Sul, "Analysis on output LC filters for PWM inverters," in *Proc. IEEE 6th Int. Power Electron. Motion Control Conf.*, Wuhan, China, May 2009, pp. 384–389.

[18] Y. Liu, M. Huang, H. Wang, X. Zha, J. Gong, and J. Sun, "Reliability-oriented optimization of the LC filter in a buck DC-DC converter," *IEEE Trans. Power Electron.*, vol. 32, no. 8, pp. 6323–6337, Aug. 2017.

[19] Q. Bian, B. Nener, and X. Wang, "A modified NSGA-II for solving control allocation optimization problem in lateral flight control system for large aircraft," *IEEE Access*, vol. 7, pp. 17696–17704, 2019.

[20] A. Sundaram, "Combined heat and power economic emission dispatch using hybrid NSGA II-MOPSO algorithm incorporating an effective constraint handling mechanism," *IEEE Access*, vol. 8, pp. 13748–13768, 2020.

[21] S. Bandyopadhyay, S. Saha, U. Maulik, and K. Deb, "A simulated annealing-based multiobjective optimization algorithm: AMOSA," *IEEE Trans. Evol. Comput.*, vol. 12, no. 3, pp. 269–283, Jun. 2008.

[22] Q. Xu, Z. Xu, and T. Ma, "A survey of multiobjective evolutionary algorithms based on decomposition: Variants, challenges and future directions," *IEEE Access*, vol. 8, pp. 41588–41614, 2020.

[23] S. Bandyopadhyay, S. K. Pal, and B. Aruna, "Multiobjective GAs, quantitative indices, and pattern classification," *IEEE Trans. Syst., Man Cybern. B, Cybern.*, vol. 34, no. 5, pp. 2088–2099, Oct. 2004.

[24] M. Zhang and Y. Li, "Multi-objective optimal reactive power dispatch of power systems by combining classification-based multi-objective evolutionary algorithm and integrated decision making," *IEEE Access*, vol. 8, pp. 38198–38209, 2020.

[25] N. Kondrath and M. K. Kazimierczuk, "Inductor winding loss owing to skin and proximity effects including harmonics in non-isolated pulse-width modulated DC–DC converters operating in continuous conduction mode," *IET Power Electron.*, vol. 3, no. 6, p. 989, 2010.

[26] J. Reinert, A. Brockmeyer, and R. W. A. A. De Doncker, "Calculation of losses in ferro-and ferrimagnetic materials based on the modified Steinmetz equation," *IEEE Trans. Ind. Appl.*, vol. 37, no. 4, pp. 1055–1061, Aug. 2001.

[27] M. R. Banaei and H. A. F. Bonab, "A high efficiency nonisolated buck–boost converter based on ZETA converter," *IEEE Trans. Ind. Electron.*, vol. 67, no. 3, pp. 1991–1998, Mar. 2020.

[28] X. Lu and H. Wang, "A highly efficient multifunctional power electronic interface for PEV hybrid energy management systems," *IEEE Access*, vol. 7, pp. 8964–8974, 2019.

[29] K. Deb, A. Pratap, S. Agarwal, and T. Meyarivan, "A fast and elitist multiobjective genetic algorithm: NSGA-II," *IEEE Trans. Evol. Comput.*, vol. 6, no. 2, pp. 182–197, Apr. 2002.

[30] *Toroidal Inductor, MCAP Series*, Multicomp, MCAP115018077A-561LU Datasheet, Feb. 2020.

[31] *Aluminum Electrolytic Capacitors*, Panasonic, ECA1JM331 Datasheet, Dec. 2019.

XINZE LI (Student Member, IEEE) received the bachelor's degree in electrical engineering and its automation from Shandong University, China, in 2018. He is currently pursuing the Ph.D. degree with the School of Electrical and Electronic Engineering, Nanyang Technological University, Singapore.

His research interests include parameter design of dc–dc converter, applications of evolutionary algorithms, and deep learning algorithms in power electronics.

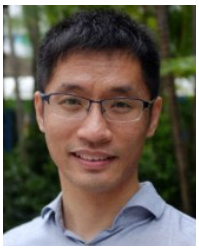

XIN ZHANG (Senior Member, IEEE) received the Ph.D. degree in electronic and electrical engineering from the Nanjing University of Aeronautics and Astronautics, China, in 2014, and the Ph.D. degree in automatic control and systems engineering from The University of Sheffield, U.K., in 2016.

From February 2017 to December 2020, he was an Assistant Professor of Power Engineering with the School of Electrical and Electronic Engineering, Nanyang Technological University, Singapore. He is currently a Professor with Zhejiang University. His research interests include power electronics, power systems, and advanced control theory, together with their applications in various sectors.

Dr. Zhang received the Highly Prestigious Chinese National Award for Outstanding Students Abroad, in 2016. He is an Associate Editor of IEEE TRANSACTIONS ON INDUSTRIAL ELECTRONICS (TIE), IEEE JOURNAL OF EMERGING AND SELECTED TOPICS IN POWER ELECTRONICS (JESTPE), IEEE OPEN JOURNAL OF POWER ELECTRONICS (OJPE), IEEE ACCESS, and *IET Power Electronics*.

FANFAN LIN (Student Member, IEEE) was born in Fujian, China, in 1996. She received the bachelor's degree in electrical engineering from the Harbin Institute of Technology, China, in 2018. She is currently pursuing the Ph.D. degree with Nanyang Technological University, Singapore. Her research interest includes the power converter design with artificial intelligence.